#### 5.2.2.3 Synthesis of rGO/Sodium Silicate Composites

The sodium silicate has been already introduced in chapter 3 as a possible low cost, environmentally friendly material for the reduction of the graphene oxide. In this section graphene sheets as conductive filler are combined in a sodium silicate gel network and the sodium ions are used as conductive ions species of the device, going towards more environmentally friendly, cheaper and safer electrochemical devices. The goal of this experiments is to achieve an in situ reduction of the graphene oxide and the synthesis of a possible material to use as electrode material for sodium based supercapacitor applications.

**Materials and Methods** The chemicals used were: sodium silicate solution, $Na_2O$:$SiO_2$ = 1:3.33), citric acid and $Na_2SO_4$ purchased from Sigma-Aldrich, graphene oxide purchased from ACS Materials (USA). Deionized (DI) water was used as a solvent for the electrolyte. A solution of 50 mg of sodium metasilicate in 0.5 ml of DI water was obtained by heating the solution on a hot plate at $80^oC$ for 5 minutes under stirring with a magnetic bar. Dispersions of graphene oxide in DI water were obtained under mild sonication (25 W, 40 KHz) for a total volume of 0.5 ml and a concentration of graphene oxide of 0.5 mg/ml.
The graphene oxide dispersion was then added to the sodium silicate solution in order to obtain a 1.05 equivalent of the solution of sodium silicate in water, and put on the hot plate at $95^oC$ for 10-15 minutes. Silica hydrosols were prepared by adding 3 M citric acid drop by drop to the GO/sodium silicate solution of 1.05 specific gravity while stirring for 5 minutes and kept for gelation in a temperature controlled oven. After gelation, the gels were aged for 3 h at $50^oC$ to strengthen the gel network.

**Results and Discussion** In acidic solution the silicate ions react with hydrogen ions and they form the acidic acid, that forms silica gel a hard and glassy substance. The gel structure is composed by $SiO_2$ and sodium ions floating in it and possibly they can be part of the ionic conductivity in an electrochemical system.

The starting pH of the GO/Sodium silicate dispersion was of 12 and through the addition of the citric acid the pH dropped to 10.33, pH at which is starting the gelation process and creating a network of $SiO_2$ with sodium ions floating in the gel structure as showed in Figure 5.32.

The pH value is critical for the gelation of the sodium silicate because if the pH drops lower

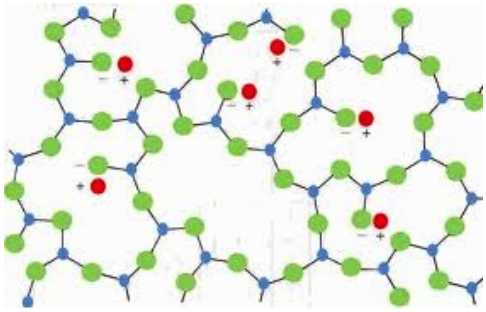

Figure 5.32 Sodium silicate gel chemical structure after gelation.

the reaction does not occur. The citric acid was preferred to for example the hydrochloridric acid for timing of the gelation time, in fact as reported in Figure 5.33 the citric acid has a slower gelation time that gives the possibility of better control the sample preparation and at the same time has a relatively low percentage of the volume shrinkage. In Figure 5.34 and

| Concen-tration of acid (M) | Gelation time (min.) | Volume shrin-kage (%) | Poro-sity (%) | Pore volume (cc/g) | Thermal conductivity (W/m.K) | Contact angle (deg.) |
|---|---|---|---|---|---|---|
| **Hydrochloric acid (HCl)** | | | | | | |
| 1 | 19,920 | 95 | 95 | 10.0 | 0.100 | <90 |
| 2 | 1,470 | 91 | 85 | 2.9 | 0.150 | <90 |
| 3 | 10 | 86 | 84 | 2.8 | 0.151 | 135 |
| 4 | 5 | 77 | 87 | 3.6 | 0.137 | 138 |
| 5 | 5 | 73 | 89 | 4.4 | 0.118 | 145 |
| **Citric acid ($C_6H_8O_7.H_2O$)** | | | | | | |
| 1 | 315 | 82 | 89 | 4.2 | 0.121 | 145 |
| 2 | 2 | 77 | 87 | 3.6 | 0.127 | 143 |
| **3** | **20** | **34** | **95** | **11** | **0.092** | **148** |
| 4 | 45 | 39 | 95 | 9.9 | 0.100 | 148 |

Figure 5.33 Sodium silicate gel conditions.

Figure 5.35 are shown two sample of sodium silicate gel and sodium silica gel with graphene

oxide as a filler. The gels were prepared adding 0.35 g of sodium silicate in 5.5 g of DI Water and for the GO composite also 7.5 mg of GO, with a initial pH of 13.50, to which has been added 1.1 ml of 3 M citric acid while stirring until a pH of 10.33. Finally were transferred in the oven at 50$^o$C for 1 hour. Aging tests were also performed in order to verify the

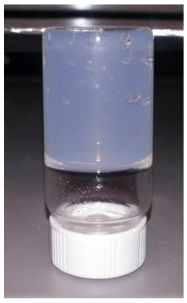

Figure 5.34 Sodium silicate gel.

Figure 5.35 Sodium silicate gel with graphene oxide as a filler.

shrinkage percentage, and after 24 hours in air the gel becomes dry solid and fragile by loosing all the water; solubility test were also performed in order to verify the non solubility in the electrolyte solution use for electrochemical test, the samples were immersed in 2M $Na_2SO_4$ of solution in DI water and after one hour aging the silica gel structure didn't lose it shape also if heated at 200$^o$C eventually becoming stone solid.

In order to complete the electrochemical characterizations the electrode were prepared directly on the metal grid, following the process described in Figure 5.36, where the metal mesh was already put in the vial with a magnetic bar for stirring the solution during the gelation, keeping the solution at an homogeneous value of pH. The grid with the gel formed on top was then transferred in a vacuum oven at 50$^o$C for 1 hour and rinsed with DI Water. In Figure 5.37


Figure 5.36 Electrode assembling process scheme.

are showed the GO/sodium silicate electrode at different stage of the process, the gel and gel/carbon stayed on the grids also after aging and washing with DI water loosing part of their volume due to the water evaporation. To date, this non-toxic rGO/sodium silicate composite

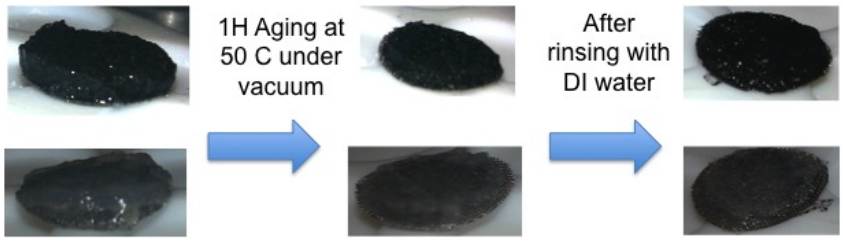


Figure 5.37 Pictures of GO/sodium silicate electrodes gel on metal grid after aging and washing processes.

has not been explored for the preparation of electrodes for energy storage, for this reason cyclic voltammetry measurements were also performed on sodium silicate and GO/sodium silicate composite electrodes in order to verify the feasibility. In Figure 5.38 and Figure 5.39 are reported the data obtained at 50 and 100 mV/s in a voltage window of -0.5V to +0.5V.
The curves have similar amplitude in current, the values are in both case very low and so are the specific capacitance values, not even comparable with previous reported values. For what concern the shape of the curves it is noticeable that a more squared shape in the GO/sodium silicate composite sign of a more capacitive behavior compared to the pure sodium silicate gel possibly due to the higher surface area introduced by the graphene.

## 5.3 Conclusion

In conclusion, highly porous graphene hybrid composites were prepared using environmentally friendly, low cost and safe material and processes. Among all the materials investigated the best candidate to become an electrode material for sodium based supercapacitors has been

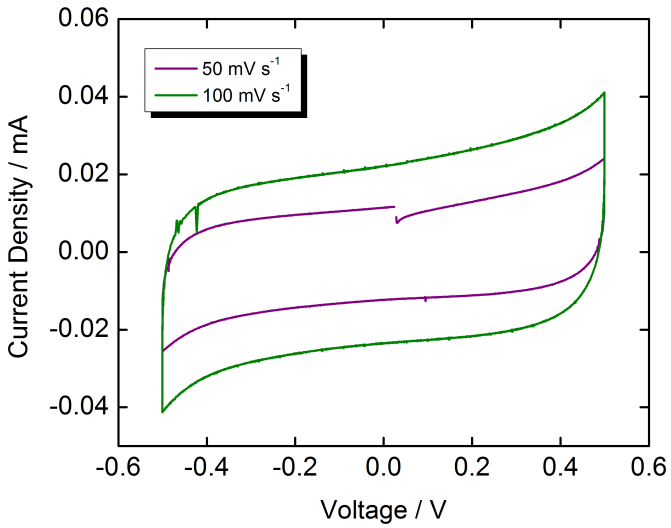


Figure 5.38 Cyclic voltammetry of sodium silicate gel electrodes at 50 and 100 mV/s in a voltage window of -0.5V to +0.5V.

the composite graphene/molybdenum dioxide obtained through a facile one-pot hydrothermal synthesis. Structural characterization indicates the formation of polycrystalline nanoparticles of $MoO_2$ on reduced graphene oxide surface. The molybdenum oxide of the hybrid facilitates redox reaction associated with Na+ ion insertion in aqueous electrolyte. And the ion insertion behavior is not fully reversible even though there were no apparent changes in the crystal structures of $MoO_2$. The fact that the hybridization lowers impedance and increases the specific capacity is intriguing for designing better supercapacitor using RGO-metal oxide hybrid electrodes. Another interesting composite was obtained from the combination of graphene oxide and expanded graphite. This composite reached similar specific capacitance values compared to the electrodes with just GO and this result can made this combination a good candidate for the use in EDLC supercapacitors, lowering the overall cost of the electrodes. The composites with the sodium silicate have been an interesting study from the point of view of an alternative way of graphene oxide reduction, but the values of specific capacitance obtained are not enough high to make it a possible material for supercapacitors applications.

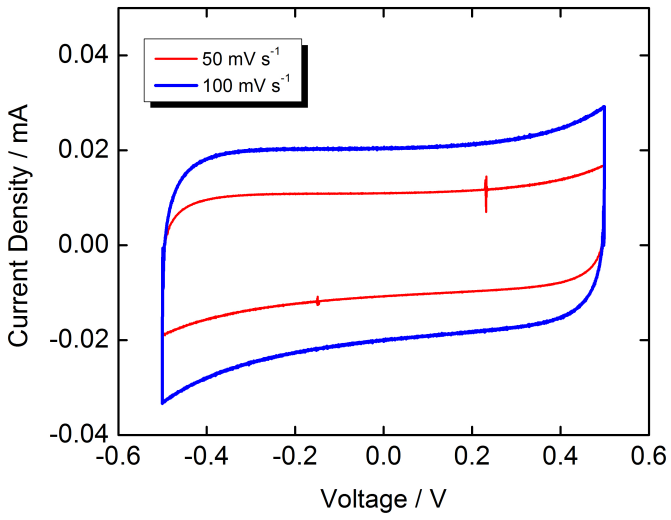


Figure 5.39 Cyclic voltammetry of RGO/sodium silicate gel electrodes at 50 and 100 mV/s in a voltage window of -0.5V to +0.5V.

# Chapter6. CONCLUSIONS AND FUTURE WORKS

The goal of this dissertation was to prove the possibility and the feasibility of obtaining graphene based hybrids for high performance devices through the use of environmentally friendly and safe materials and processes, keeping always in mind the importance of lowering the overall cost of production of the final devices and the easy manufacturing.

In chapter 2 graphene direct exfoliation synthesis methods have been investigated and discussed. It was demonstrate that few layer graphene, with a number of layers that ranges between two and five, can be prepared by direct sonication of the expanded graphite in ionic liquids solutions. This method is considered simple and green, because it avoids oxidation and subsequent reduction steps if compared to standards methods, like the Hummers method. The suitable surface tensions and ionic feature facilitate the exfoliation of graphite and the imidazolium based ionic liquid and helps the stabilization of the few layer graphene, according a high concentration of suspension. It is possible to conclude that this process can be considered as a possible environmentally friendly, simple and fast method for the exfoliation of the graphite and the synthesis of few layer graphene.

Unfortunately, the synthesis yields obtained by direct exfoliation is not yet comparable with the more standard processes, and for large production of graphene chemical ways, through the oxidation of the graphite, are still the most employed. For this reason reduction methods, in order to obtain reduced graphene oxide, are necessary and in chapter 3, three methods concerning UV-light, hydrothermal and chemical reduction of the graphene oxide have been investigated. These methods have in common low cost, low power consumption, simplicity and non toxicity aspects on top of being very efficient in the reduction of the graphene oxide. The characteristics of these methods are interesting and in this dissertation all of them have been used in the synthesis process of graphene based composite materials, for important applications

as printed flexible electronics and electrodes for energy storage devices.

The use of the graphene for printed flexible electronics applications has been investigated in chapter 4, and a route to obtain inkjet printable, environmentally friendly inks based on graphene/acrylic nanocomposites using water as solvent, was presented and discussed in detail. The concurrent UV-driven polymerization of PEGDA matrix, chosen for its non toxicity and water solubility properties, and the reduction of graphene oxide filler was verified by XPS analysis and thin printed samples of the nanocomposite showed a decrease of resistivity by two orders of magnitude with respect to the pure matrix because of the excellent conductivity properties of the graphene used as a conductive filler in the polymer matrix. It was also discovered that the reduction of the graphene oxide through UV-light exposure is proportional to the amount of incoming light, therefore it is more effective in thin layers, where the light penetration is higher than in thick layers. As the excellent rheological characteristics of the formulations warranted printability with good repeatability, suggested applications for the so-prepared inks can be devoted to flexible and organic electronics as for example, the realization of an electrode on top of a stacked structure (e.g., an active device such as a transistor or a photovoltaic cell) made out of organic semiconductor materials.

This graphene/polymer composite can be deposited at room temperature and it is a very important aspect since metal nanoparticle-based inks instead require sintering thermal treatments which are not compatible with organic materials. A conductive ink ready to be structured by an additive process like inkjet printing and needing only a fast post-deposition treatment like UV curing is very interesting also from an industrial point of view. Further work would explore the possibility of formulating graphene-based printable inks using different polymeric matrices such as intrinsically conductive polymers, whose printability has already been demonstrated, with extremely interesting electrical properties (152), (153) and the incorporation of metal nanoparticles or carbon nanotubes, to increase the percolation and reduce the ultimate resistivity.

Another application of graphene composite materials used as electrodes for energy storage devices, the supercapacitors, was investigated in chapter 5. Highly porous graphene hybrid composites were prepared using environmentally friendly, low cost and safe material and processes.

Among all the composites investigated the best candidate to become an electrode material for sodium based supercapacitors has been demonstrate to be the graphene/molybdenum dioxide composite, obtained throught a facile one-pot hydrothermal synthesis. The molybdenum oxide of the hybrid facilitates redox reaction associated with Na+ ion insertion in aqueous electrolyte reaching the high value of 381 F/g for the specific capacitance. The fact that the composite not only increases the specific capacity but lowers also the equivalent series resistance values respect to the graphene oxide only, it is intriguing for designing better supercapacitor using RGO/metal oxide hybrid electrodes. Another interesting composite was obtained from the combination of graphene oxide and expanded graphite. This composite was obtained again through the use of the hydrothermal synthesis and it is able to reach similar specific capacitance values compare to electrodes with just the graphene oxide and this result can made this combination a good candidate for EDLC supercapacitors, in particular to lower the overall cost of the electrodes.
Finally a composite of graphene oxide and sodium silicate gel has been investigated with the idea of obtaining an electrode material with already integrated sodium ions in a 3D structure of $SiO_2$ with the graphene as conductive filler. The presence of an abundant material like the $SiO_2$ could be a good solution to lower the cost of production and in addition, the reduction of the graphene oxide during the gelation process has been also demonstrated. Unfortunately, the values of specific capacitance obtained from the electrochemical measurements were not enough to make it a possible material for supercapacitors applications and future work could involve the optimization of this composite in order to increase the surface area and subsequently the specific capacitance, by possibly incorporating graphene 3D structures previously obtained with the hydrothermal synthesis.
The results presented in this dissertation is a good starting point for very interesting future works. For example, the liquid electrolyte of the supercapacitor could be substitute by a polymer electrolyte mixed with ionic species, in order to obtain a novel sodium based solid state supercapacitor; ink jet printing or additive manufacturing techniques could be also employed for the realization of the final device, in order to achieve different electrode shapes and be able to print devices also on flexible substrates for possible wearable applications.

# APPENDIX A. CHARACTERIZATION METHODS

The intention of this chapter is to provide a brief overview of all the characterization techniques that have been employed in this dissertation for the study of the materials and devices. The characterizations described in this chapter are organized in three general groups: morphological, compositional and electrochemical. The morphological characterizations that have been used in the study of the graphene and the its composites were employed to obtain informations regarding the dimentions, the shapes and the surface morphology; the main characterizations that have been employed include optical microscope, for a qualitative low resolution analysis, scanning electron mycroscopy for a more detailed and high resolution morphologycal analysis in the submicron range, profilometer for a obtain an estimation of the thickness of macro structures from hundreds of micron to millimiters and atomic force microscopy in order to obtain information regarding the thickness of the micro/nano materials and an estimation of the surface roughtness. Transmission electron microscopy has also been employes for the high resolution imaging of the samples and the characterization of crystalline planes.

Compositional characterizations have been also employed for a deep understanding of the materials and the composites. Several spectroscopy techniques have been employed for the samples characterization including Raman, energy dispersive X-Ray, electron energy loss and X-ray photoelectron spectroscopy are going to be presented together with X-ray diffraction, used for the detection of crystallinity phase, elemental composition of the composite materials and for the lattice paramenters modification occurring in the different reactions. In the end are going to be presented the electrochemical tecniques used for the characterization of the graphene composites to evaluate the possibility of using them for the applications that are under study.

## A.1 Morphological Characterizations

**Optical Microscopy** Optical microscope is a type of microscope which uses visible light and a system of lenses to magnify images of small samples. It is usually used for a rapid analysis of the wafers anfter the CVD or epitassial growth of the graphene to have rapid information on the homogenity of the growth on large areas. For what concerns the graphene obtained by expholiation process, a specific $SiO_2$ wafer is emploied to be able to discriminate the difference in thickness of the different flakes (204); in fact, the wafer usually used is the 300 nm $SiO_2$ on silicon and in chapter 3 is explained an efficient method, called the "meniscus" method, to deposit large quantities of graphene flakes on the substrate avoiding their restacking and agglomeration. The thickess of the oxide allow to see the few layers graphene flakes in different colors, depending on their thickness due to the different refraction of the light (205).

**Profilometer** The profilometer is a direct technique because no modeling is required. The instrument is used to measure a surface's profile, in order to quantify its roughness. A diamond stylus is moved vertically in contact with a sample and then moved laterally across the sample for a specified distance and specified contact force. A profilometer can measure small surface variations in vertical stylus displacement as a function of position. A typical profilometer can measure small vertical features ranging in height from 10 micrometers to 1 millimeter. The height position of the diamond stylus generates an analog signal which is converted into a digital signal stored, analyzed and displayed. Contacting the surface is often an advantage in dirty environments where non-contact methods can end up measuring surface contaminants instead of the surface itself. Because the stylus is in contact with the surface, this method is not sensitive to surface reflectance or color. In this dissertation the profilomenter has been presented in order to detect ink ket printed tracks thickness and roughness (206).

**Atomic Force Microscopy (AFM)** AFM system under ambient conditions in tapping mode with a standard 300 kHz silicon tapping tip (BudgetSensors, radius 10nm) has been em-

ploied for the graphene sheets analysis. AFM is a very high-resolution type of scanning probe microscopy, with demonstrated resolution on the order of fractions of a nanometer. The AFM is one of the foremost tools for imaging, measuring, and manipulating matter at the nanoscale. The information is gathered by "feeling" the surface with a mechanical probe. The AFM consists of a cantilever with a sharp tip (probe) at its end that is used to scan the specimen surface. The cantilever is typically silicon or silicon nitride with a tip radius of curvature on the order of nanometers. When the tip is brought into proximity of a sample surface, forces between the tip and the sample lead to a deflection of the cantilever according to Hooke's law (207). AFM is largely ued to detect the presence of graphene sheets when the substrate doesn't have the right optical properties. AFM is a non destrictive tecniques that scan the surface of the sample giving topographic informations giving dateiled informations on the shape, the height roughtness and phase of the graphene sheets (208).

**Scanning Electron Microscopy (SEM)** SEM analysis was done with a FEI Helios Nanolab 400S field emission FIB/SEM. SEM is a type of electron microscope that produces images of a sample by scanning it with a focused beam of electrons. The electrons interact with atoms in the sample, producing various signals that can be detected and that contain information about the sample's surface topography and composition.The most common mode of detection is by secondary electrons emitted by atoms excited by the electron beam. On a flat surface, the plume of secondary electrons is mostly contained by the sample, but on a tilted surface, the plume is partially exposed and more electrons are emitted. By scanning the sample and detecting the secondary electrons, an image displaying the topography of the surface is created. SEM is used to investifate the structure and number of the graphene sheets (214). In face it is a valid characterization for samples highly porous giving the possibility to explore the structure that otherwise with the AFM would be impossible to analyse due to the roughtness and thickness of the sample (217).

**Transmission Electron Microscopy (TEM)** A JEOL JEM-ARM200F STEM Cs-corrected cold FEG (Field Emission Gun) atomic resolution analytical microscope with GIF Quantum post column energy filter and JEOL Centurio SDD EDS (silicon drift detector energy dispersive spectrometer) was used for Transmission Electron Microscopy analysis. TEM is a microscopy technique in which a beam of electrons is transmitted through an ultra-thin specimen, interacting with the specimen as it passes through. An image is formed from the interaction of the electrons transmitted through the specimen; the image is magnified and focused onto an imaging device, such as a fluorescent screen, on a layer of photographic film, or to be detected by a sensor such as a CCD camera. TEM has been employed for the study of the crystalline structure of the graphene flakes (209), (218) in the study of the crystallinity of the compoud create with the graphene and with a local EDS was also possible to investigate the elements composition of the sample in analysis.

## A.2 Compositional Characterizations

**Raman Spectroscopy** Raman spectra were collected using a Renishaw system 1000 Raman spectrometer equipped with an integral microscope (Leica DMLMS/N). Excitation was provided by a 25-mW He-Ne laser and the 632.8 nm excitation beam was focused onto the sample with a 50 objective; the laser power at the sample was approximately 3 mW. The backscattered Raman light was collected with the same 50 objective and focused into a Peltier cooled charge-coupled device (CCD) camera (400  600 pixels). An edge filter removed background from the Rayleigh scattered light, while a holographic grating (1800 grooves/mm) and a 50$\mu$m slit permitted a spectral resolution of $\sim$1 cm$^1$. A silicon wafer with a Raman band at 520 cm$^1$ was used to calibrate the spectrometer and the accuracy of the spectral measurements was estimated to be better than 1 cm$^1$.

Raman Spectroscopy is a methods largely used for the characterization of the graphene and, it helps in the detection of the number of layers, disorder, doping level and all these paramenters they can be detected by a short-time measurement in ambient condition avoiding serious degradation of the graphene. The standard measurement data analysis consist in collecting the spectrum of the material and substract the spectrum of the substrate. For what concerns the carbon raman spectrum, the D peak is mediated by an elastic scattering with difects and inelastic scattering with a phonon, while the 2D peak is medited by two inelastic scatterings and it is more sensitive tho the electronic structure of the graphene and it is possible to distinguish a monolayer from a few layer graphene analysing the 2D peak (210).

**X-Ray Photoelectron Spectroscopy (XPS)** XPS is a surface-sensitive quantitative spectroscopic technique that measures the elemental composition that can be used to analyze the surface chemistry of a material in its as-received state. XPS spectra are obtained by irradiating a material with a beam of X-rays while simultaneously measuring the kinetic energy and number of electrons that escape from the top 0 to 10 nm of the material being analyzed. The XPS analysis performed on all the experiments presented in this dissertation are performed using a Physical Electronics Quantum ESCA Microprobe, using a monochromated Al K$\alpha$ X-ray

source, 200 mm spot size throughout and charge neutralization, and 1000 eV survey spectra (187 eV pass energy, 1.6 eV/step) and high resolution spectra (47 eV PE, 0.4 eV/step) were aquired. Before performing XPS, the homogeneity of the samples was verified using an in situ secondary X-ray imaging. An example of use of theis characterization technique is the study of the oxygenation state of the carbon. the peak C1s is usually analyse in depth and its deconvolution gives quantitative and qualitative informations about the functional groups present on the surface of the graphene (211), (219).

**X-Ray Diffraction (XRD)** X-ray diffraction (XRD) measurements were performed on a Bruker D8 Discover X-ray diffractometer fitted with a 2-dimensional (2D) X-ray detector. All scans were performed with the detector and incident beam in a symmetric $\theta$-$2\theta$ geometry using graphite monochromated Cu-K$\alpha$ X-rays ($\lambda = 1.5418$ Å) collimated in a pin-hole collimator to yield $\sim$650 $\mu$m diameter X-ray beam on the sample being measured. Data are collected at room temperature in the 2D mode with an integration time of at least 30 minutes for each frame. During measurements, the discharged cathode is oscillated in the x-y plane (the sample plane) with 2 mm oscillation amplitude. Therefore, the X-ray diffractograms represent a spatial average over an area of at least 4 X 4 $mm^2$ on the cathode. The collected data (at least four frames to cover a $2\theta$ range of 80 degrees) is integrated over c, the polar angle orthogonal to $2\theta$ to yield the intensity vs $2\theta$ plots shown in the manuscript. We did not find any noticeable changes in the XRD patterns over the measurement time. XRD is used for identifying the atomic and molecular structure of a crystal, in which the crystalline atoms cause a beam of incident X-rays to diffract into many specific directions. By measuring the angles and intensities of these diffracted beams, a crystallographer can produce a three-dimensional picture of the density of electrons within the crystal. From this electron density, the mean positions of the atoms in the crystal can be determined, as well as their chemical bonds, their disorder and various other information (212), (213).

**Electron Energy Loss Spectroscopy (EELS)** All Electron Energy Loss Spectroscopy (EELS) spectra were taken at 1eV/channel dispersion and GIF was used to collect EELS. Using a EELS a material is exposed to a beam of electrons with a known, narrow range of kinetic energies. Some of the electrons will undergo inelastic scattering, which means that they lose energy and have their paths slightly and randomly deflected. The amount of energy loss can be measured via an electron spectrometer and interpreted in terms of what caused the energy loss. Inelastic interactions include phonon excitations, inter and intra band transitions, plasmon excitations, inner shell ionizations, and Cherenkov radiation. The inner-shell ionizations are particularly useful for detecting the elemental components of a material. EELS has historically been a difficult technique but is in principle capable of measuring atomic composition, chemical bonding, valence and conduction band electronic properties, surface properties, and element-specific pair distance distribution functions (216), EELS tends to work best at relatively low atomic numbers, where the excitation edges tend to be sharp, well-defined, and at experimentally accessible energy losses.

**Energy Dispersive X-Ray Spectroscopy (EDX)** EDX analysis was done with a FEI Helios Nanolab 400S field emission FIB/SEM with a Bruker Quantax 200 EDX detector. EDX excels at identifying the atomic composition of a material, is quite easy to use, and is particularly sensitive to heavier elements. It is an analytical technique used for the elemental analysis or chemical characterization of a sample and it relies on an interaction of some source of X-ray excitation and a sample. Its characterization capabilities are due in large part to the fundamental principle that each element has a unique atomic structure allowing unique set of peaks on its X-ray emission spectrum (215). The incident beam may excite an electron in an inner shell, ejecting it from the shell while creating an electron hole where the electron was. An electron from an outer, higher-energy shell then fills the hole, and the difference in energy between the higher-energy shell and the lower energy shell may be released in the form of an X-ray. The number and energy of the X-rays emitted from a specimen can be measured by an energy-dispersive spectrometer. As the energy of the X-rays are characteristic of the differ-

ence in energy between the two shells, and of the atomic structure of the element from which they were emitted, this allows the elemental composition of the specimen to be measured (215).

**Thermogravimetric Analysis (TGA)** The Thermogravimetric Analysis (TGA) used for the analysis of the graphene samples is a Q500 by TA Instruments and all the measurement were performed in air increasing the temperature 5 degree per minute. The TGA was employed to obtain an estimation of the mass of the different components in the composite materials.

## A.3 Electrical and Electrochemical Characterizations

Current/voltage (IV) measurements were performed on thick and printed films of a graphene/polymer composite obtained for printed electronic application trough the use of an ink jet printer, were performed by using a standard two point micro-contact setup of a Keithley 2635A multimeter. For electrochemical analysis needed to evaluate paremeter as specific capacitance and equivalent series resistance for possible electrode materials obtained dureing the experiments, a BioLogic multi potentiostats/galvanostats/EIS VPS-300 was used with its function of cyclic voltammetry, electron impedance spectroscopy and galvanostatic charge/discharge techniques.

**Cyclic Voltammetry (CV)** Cyclic Voltammetry (CV) is a type of potentiodynamic electrochemical measurement. In a cyclic voltammetry experiment the working electrode potential is ramped linearly versus time like linear sweep voltammetry. Cyclic voltammetry takes the experiment a step further than linear sweep voltammetry which ends when it reaches a set potential. When cyclic voltammetry reaches a set potential, the working electrode's potential ramp is inverted. This inversion can happen multiple times during a single experiment. The current at the working electrode is plotted versus the applied voltage to give the cyclic voltammogram trace. Cyclic voltammetry is generally used to study the electrochemical properties of an analyte in solution. If the redox couple is reversible then when the applied potential is reversed, it will reach the potential that will reoxidize the product formed in the first reduc-

tion reaction, and produce a current of reverse polarity from the forward scan. This oxidation peak will usually have a similar shape to the reduction peak. As a result, information about the redox potential and electrochemical reaction rates of the compounds are obtained. It is widely used to study a variety of redox processes, for obtaining stability of reaction products, the presence of intermediates in oxidation-reduction reactions, reaction and electron transfer kinetics, and the reversibility of a reaction.

**Electron Impedance Spectroscopy (EIS)** Electron Impedance Spectroscopy (EIS) measures the dielectric properties of a medium as a function of frequency. This technique measures the impedance of a system over a range of frequencies, and therefore the frequency response of the system, including the energy storage and dissipation properties, is revealed. Often, data obtained by EIS is expressed graphically in a Bode plot or a Nyquist plot. Impedance is the opposition to the flow of alternating current (AC) in a complex system. A passive complex electrical system comprises both energy dissipater (resistor) and energy storage (capacitor) elements. If the system is purely resistive, then the opposition to AC or direct current (DC) is simply resistance.

**Galvanostatic Charge/Discharge (GCD)** Galvanostatic Charge/Discharge (GCD) is the standard technique used to test the performance and cycle life of EDLCs and batteries. A repetitive loop of charging and discharging is called a cycle. Internal leakage current leads to a continuous voltage drift that discharges the cell.

# BIBLIOGRAPHY

[1] Novoselov, K. S.; Geim, A. K.; Morozov, S. V.; Jiang, D.; Zhang, Y.; Dubonos, S. V.; Grigorieva, I. V.; Firsov, A. A. (2004) Electric Field Effect in Atomically Thin Carbon Films. *Science*, *306*, 666–669.

[2] Geim, A. K. (2009) Graphene: Status and Prospects. *Science*, *324*, 1530–1534.

[3] Stankovich, S.; Dikin, D. A.; Dommett, G. H. B.; Kohlhaas, K. M.; Zimney, E. J.; Stach, E. A.; Piner, R. D.; Nguyen, S. T.; Ruoff, R. S. (2006) Graphene-Based Composite Materials. *Nature*, *442*, 282–286.

[4] Li, X. L.; Wang, X. R.; Zhang, L.; Lee, S. W.; Dai, H. J. (2008) Chemically Derived, Ultrasmooth Graphene Nanoribbon Semiconductors. *Science*, *319*, 1229–1232.

[5] Balandin, A. A.; Ghosh, S.; Bao, W. Z.; Calizo, I.; Teweldebrhan, D.; Miao, F.; Lau, C. N. (2008) Superior Thermal Conductivity of Single-Layer Graphene. *Nano Lett.*, *8*, 902–907.

[6] Lee, C.; Wei, X. D.; Kysar, J. W.; Hone, J. (2008) Measurement of the Elastic Properties and Intrinsic Strength of Monolayer Graphene. *Science*, *321*, 385–388.

[7] Kim, K. S.; Zhao, Y.; Jang, H.; Lee, S. Y.; Kim, J. M.; Ahn, J. H.; Kim, P.; Choi, J. Y.; Hong, B. H. (2009) Large-Scale Pattern Growth of Graphene Films for Stretchable Transparent Electrodes. *Nature*, *457*, 706–710.

[8] Park, S.; Ruoff, R. S. (2009) Chemical Methods for the Production of Graphenes. *Nat. Nanotechnol.*, *4*, 217–224.

[9] Choi W., Lee J. W. Graphene: Synthesis and Applications. *CRC Press*, ISBN-13: 978–1439861875.

[10] I. A. Ovidko (2013) Mechanical properties of graphene. *Rev.Adv. Mater. Sci.*, *34*, 1–11.

[11] Geim A.K., K.S. Novoselov (2007), The rise of the Graphene *Nature*, *6*, 183–191.

[12] Reddy D., RegisterL.F., Carpenter G. D., BanerjeeS. K. (2011) Graphene field-effect transistors. *Journal of Physics D*, *44*.

[13] Meric I., Han M. Y., Young A. F., Ozyilmaz B., Kim P., Shepard K. L. (2008) Current saturation in zero-bandgap, top-gated graphene field-effect transistors *Nature Nanotechnology*, *3*, 654–659.

[14] Tang Z. (2010) Constrant of DNA on functionalized graphene improves its biostability and specificity. *Small*, *6*, 1205–1209.

[15] Schedin F. (2007) Detection of individual gas molecules adsorbed on graphene. *Nature materials*, *6*, 652–655.

[16] Fowler, J. D.; Allen, M. J.; Tung, V. C.; Yang, Y.; Kaner, R. B.; Weiller, B. H. ( 2009) Practical Chemical Sensors from Chemically Derived Graphene. *ACS Nano*, *3*, 652–655.

[17] Lu, C. H.; Yang, H. H.; Zhu, C. L.; Chen, X.; Chen, G. N. A (2009) Graphene Platform for Sensing Biomolecules. *Angew. Chem., Int. Ed.*, *48*, 4785–4787.

[18] Shan, C. S.; Yang, H. F.; Song, J. F.; Han, D. X.; Ivaska, A.; Niu, L. (2009) Direct Electrochemistry of Glucose Oxidase and Biosensing for Glucose Based on Graphene. *Anal. Chem.*, *81*, 2378–2382.

[19] Li X., Zhu Y., Cai W., Borysiak M., Han B., Chen D., Piner R. D., Colombo L., Ruoff R. S. (2009) Transfer of Large-Area Graphene Films for High-Performance Transparent Conductive Electrodes *Nano Lett.*, *9*(12), 4359–4363.

[20] Xu, Y. X.; Hong, W. J.; Bai, H.; Li, C.; Shi, G. Q. (2009) Strong and Ductile Poly(vinyl alcohol)/Graphene Oxide Composite Films with a Layered Structure. *Carbon*, *47*, 3538–3543.

[21] Ramanathan, T.; Abdala, A. A.; Stankovich, S.; Dikin, D. A.; Herrera-Alonso, M.; Piner, R. D.; Adamson, D. H.; Schniepp, H. C.; Chen, X.; Ruoff, R. S.; et al. Functionalized Graphene Sheets for Polymer Nanocomposites. 2008 *Nat. Nanotechnol.*, *3*, 327–331.

[22] Hong, W. J.; Xu, Y. X.; Lu, G. W.; Li, C.; Shi, G. Q. Transparent Graphene/PEDOT-PSS Composite Films as Counter Electrodes of Dye-Sensitized Solar Cells. 2008 *Electrochem. Commun.*, *10*, 1555–1558.

[23] Wang, Y.; Shi, Z. Q.; Huang, Y.; Ma, Y. F.; Wang, C. Y.; Chen, M. M.; Chen, Y. S. (2009) Supercapacitor Devices Based on Graphene Materials. *J. Phys. Chem. C*, *113*, 13103–13107.

[24] Qu, L. T.; Liu, Y.; Baek, J. B.; Dai, L. M. (2010) Nitrogen-Doped Graphene as Efficient Metal-Free Electrocatalyst for Oxygen Reduction in Fuel Cells. *ACS Nano*, *4*, 1321–1326.

[25] Hoffman H. Flexible, Printed Electronics At the Tipping Point. *FlexTech Alliance*, http://www.semi.org/en/node/48211.

[26] Klauk H (2007). *Nat Mater*, *6*, 397.

[27] Singh M, Haverinen HM, Dhagat P, Jabbour EG (2010). *Adv Mat*, *22*, 673.

[28] De Gans BJ, Duineveld PC, Schubert US (2004). *Adv Mat*, *16*, 203.

[29] Perelaer J, Smith PJ, Mager D, Soltman D, Volkman SK, Subramanian V, Korvinkdf JG, Schubert US (2010). *J Mater Chem*, *20* (39), 8446.

[30] Cho J, Shin K, Jang J (2010). *Thin Solid Films*, *518*, 5066.

[31] Park BK, Kim D, Jeong S, Moon J, Kim JS (2007). *Thin Solid Films*, *515*, 7708.

[32] Chiolerio A, Cotto M, Pandolfi P, Martino P, Camarchia V, Pirola M, Ghione G (2012). *Microelectron Eng*, *97*, 8.

[140] Denneulin A, Bras J, Carcone F, Neuman C, Blayo A (2011). *Carbon*, *49*, 2603.

[141] Luechinger NA, Athanassiou EK, Stark WJ (2008). *Nanotechnol*, *19*, 445201.

[35] Shin KY, Hong JY, Jang J (2011). *Adv. Mater.*, *23*, 2113.

[36] Novoselov KS, Geim AK, Morozov SV, Jiang D, Katsnelson MI, Grigorieva IV, Dubon SV, Firsov AA (2005). *Nature*, *438*, 197.

[37] Novoselov KS, Jiang Z, Zhang Y, Morozov SV, Stormer HL, Zeitler U, Mann JC, Boebinger GS, Kim P, Geim AK (2007). *Science*, *315*, 1379.

[38] BP Statistical Review of World Energy, (2014) www.bp.com/statisticalreview.

[39] U.S. Energy Information Administration (EIA) (2013) International Energy Outlook. http://www.eia.gov/forecasts/ieo/pdf/0484(2013).pdf

[156] Shukla AK, Banerjee A, Ravikumar MK, Jalajakshi A. (2012) Electrochemical capacitors: technical challenges and prognosis for future markets. *Electrochimica Acta*, *84*, 165–173.

[41] TU.S. Department of Energy, (2007) Basic Research Needs for Electrical Energy Storage. www.sc.doe.gov/bes/reports/abstracts.html

[42] Simon P, Gogotsi Y. (2008) Materials for electrochemical capacitors. *Nature Materials*, *7*, 845–854.

[43] M.J. Allen, V.C. Tung, R.B. Kaner, (2010). *Chem. Rev.*, *110*, 132.

[44] Reina A., Jia X., Ho J., Nezich D., Son H., Bulovic V., Dresselhaus M. S., Kong J. (2009) *Nano Lett.*, *9* (1), 30–35.

[45] Li X., Cai W., An J., Kim S., Nah J., Yang D., Piner R., Velamakanni A., Jung I., Tutuc E.,Banerjee S. K., Colombo L., Ruoff R.S. (2009) Large-area synthesis of high quality and uniform graphene films on copper foils. *Science*, *324* (5932), 1312–1314.

[46] M. Eizenberg, J. M. Blakely, (1970). *Surf. Sci.*, *82*, 228.

[47] C. Berger, Z. Song, X. Li, X. Wu, N. Brown, C. Naud, D. Mayou, T. Li, J. Hass, A. N. Marchenkov, E. H. Conrad, P. N. First and W. A. de Heer, (2006). *Science*, *312*, 1191.

[48] Obraztsova A. N. (2007) Chemical vapor deposition of thin graphite films of nanometer thickness. *Carbon*, *45*, 2017–2021.

[49] Coraux J. et al. 2008 Structural coherency of graphene on Ir(111] Nano letters 8(2): 565-570 *Nature Materials*, *7*, 845–854.

[50] Sutter P. W. et al. 2008 Epitaxial graphene on ruthenium. *Nature Materials*, *7*, 406–411.

[51] Zhang Y., Tan Y. W., Stormer H. L., Kim P. *Nature*, *438*, 201–204.

[52] N. Lui, F. Luo, H. Wu, Y. Liu, C. Zhang and J. Chen, (2008). *Adv. Funct. Mater.*, *18*, 1518.

[53] S. Stankovich, D. A. Dikin, R. D. Piner, K. A. Kohlhaas, A. Kleinhammes, Y. Jia, Y. Wu, S. Y. Nguyen and R. S. Ruoff, (2007). *Carbon*, *45*, 1558.

[54] Hernandez Y., Nicolosi V., Lotya M., (2008) High-yield production of graphene by liquid-phase exfoliation of graphite. *Nature Nanotechnology*, *3*, 563–568.

[55] Lotya M., Hernandez Y., King P. J., Smith R. J., Nicolosi V., Karlsson L. S., Blighe F. M., De S., Wang Z., McGovern I. T., Duesberg G. S., Coleman J. N. (2009) Liquid Phase Production of Graphene by Exfoliation of Graphite in Surfactant/Water Solutions. *J. Am. Chem. Soc.*, *131* (10), 3611–3620.

[56] William S. Hummers Jr., Richard E. Offeman (1958) Preparation of Graphitic Oxide *J. Am. Chem. Soc.*, *80* (6), 1339.

[58] Zhu J. (2008) New solutions to a new problem. *Nature nanotechnology*, *3* 528–529.

[59] Viculis LM, Mack JJ, Kaner RB. (2003) A chemical route to carbon nanoscrolls. *Science*, *299* (5611), 1361.

[60] Zhanwei Xu, Hejun Li, Wei Li, Gaoxiang Cao, Qinglin Zhang, Kezhi Li, Qiangang Fu, Jie Wang (2010) Large-scale production of graphene by microwave synthesis and rapid cooling. *Chemical Communications*, *80* (6), 1339.

[61] Liying Jiao, Li Zhang, Xinran Wang, Georgi Diankov, Hongjie Dai (2009) Narrow graphene nanoribbons from carbon nanotubes *Nature*, *458* 877–880.

[62] K S Hazra, J Rafiee, M A Rafiee, A Mathur, S S Roy, J McLauhglin, N Koratkar and D S Misra (2011) Thinning of multilayer graphene to monolayer graphene in a plasma environment *Nanotechnology*, *22* 025704.

[63] A. C. Ferrari, J. C. Meyer, V. Scardaci, C. Casiraghi, M. Lazzeri, F. Mauri, S. Piscanec, D. Jiang, K. S. Novoselov, S. Roth, and A. K. Geim, (2007), Raman Spectrum of Graphene and Graphene Layers *Phys. Rev. Lett.*, *97* 187401.

[64] Y. Xu, H. Bai, G. Lu, C. Li and G. Shi, (2008) *J. Am. Chem. Soc.*, *130* 5856.

[65] A. A. Green, M. C. Hersam, (2009). *Nano Lett.*, *9* 4031.

[66] V. Georgakilas, A. B. Bourlinos, R. Zboril, T. A. Steriotis, P. Dallas, A. K. Stubos and C. Trapalis, (2010). *Chem. Commun.*, *46* 1766.

[67] T. Welton, (1999). *Chem. Rev.*, *99* 2071.

[68] Z. Ma, J. H. Yu and S. Dai, (2010). *Adv. Mater.*, *22* 261.

[69] J. Lu, F. Yan and J. Texter, (2009). *Prog. Polym. Sci.*, *34* 431.

[70] R. D. Rogers and K. R. Seddon, Ionic Liquids: Industrial Applications to Green Chemistry, (2002). *American Chemical Society*, *818* Washington, DC.

[71] C. Chiappe and D. Pieraccini, (2005). *J. Phys. Org. Chem.*, *18* 275.

[72] T. Fukushima, A. Kosaka, Y. Ishimura, T. Yamamoto, T. Takigawa, N. Ishii, T. Aidal, (2003). *Science*, *300* 2072.

[73] X. Zhou, T. Wu, K. Ding, B. Hu, M. Hou and B. Han, (2010). *Chem. Commun.*, *46* 386.

[74] J. Restolho, J. L. Mata and B. Saramago,(2009). *J. Colloid Interface Sci.*, *340* 82.

[75] Wang X., Fulvio P. F., Baker G. A., Veith G. M., Unocic R. R., Mahurin S. M., Chib M., Dai S., (2010) Direct exfoliation of natural graphite into micrometre size few layers graphene sheets using ionic liquids. *Chem. Commun.*, *46* 4487–4489.

[76] Nuvoli D., Valentini L., Alzari V., Scognamillo S., Bittolo Bon S., Piccinini M., Illescas J., Mariani A., (2011) High concentration few-layer graphene sheets obtained by liquid phase exfoliation of graphite in ionic liquid. *J. Mater. Chem.*, *21* 3428.

[77] J. A. Harnisch, M. D. Porter, (2001). *Analyst*, *126* 1841.

[78] S. K. Reed, O. J. Lanning, P. A. Madden, (2007). *J. Chem. Phys.*, *126* 084704.

[79] Rengui Peng Polymers (2013) Progress in Imidazolium Ionic Liquids Assisted Fabrication of Carbon Nanotube and Graphene Polymer Composites. *Polymers*, *5* 847–872.

[80] S. V. Dzyuba, R. A. Bartsch, (2002). *Tetrahedron Lett.*, *43* 4657.

[81] Srinivasan Sampath, (2013) Direct Exfoliation of Graphite to Graphene in Aqueous Media with Diazaperopyrenium Dications. *Adv. Mater.*, *6* 493.

[82] Kamran Ul Hasan, Mats O Sandberg, Omer Nur and Magnus Willander, (2011) Polycation stabilization of graphene suspensions *Nanoscale Research Letters*, *6* 493.

[83] Xiaolin Li, Guangyu Zhang, Xuedong Bai, Xiaoming Sun, Xinran Wang, Enge Wang, Hongjie Dai (2008) Highly Conducting Graphene Sheets and Langmuir-Blodgett Films *Nature Nanotechnology*, *3* 538–542.

[84] Ilan Benjamin (1992) Theoretical study of the water/1,2dichloroethane interface: Structure, dynamics, and conformational equilibria at the liquidliquid interface. *J. Chem. Phys.*, *97* 1432.

[85] Z. Sun, T. Hasan, F. Torrisi, D. Popa, G. Privitera, F. Wang, F. Bonaccorso, D. M. Basko and A. C. Ferrari, (2010). *ACS Nano*, *4* 803.

[86] Kim H. J., Lee S. M., Oh Y. S., Yang Y. H., Lim Y. S., Yoon D. H., Lee C., Kim J. Y., Ruoff R. S.Unoxidized Graphene/Alumina Nanocomposite: Fracture- and Wear-Resistance Effects of Graphene on Alumina Matrix. *Scientific Reports*, *4*.

[87] Daniel R. Dreyer, Sungjin Park, Christopher W. Bielawski, Rodney S. Ruoff, (2010) The chemistry of graphene oxide *Chem. Soc. Rev.*, *39* 228–240.

[88] J. I. Paredes, S. Villar-Rodil, A. Martnez-Alonsoand, J. M. D. Tascn, (2008) Graphene Oxide Dispersions in Organic Solvents *Langmuir*, *24* (19) 0560–10564.

[89] Sungjin Park, Jinho An, Inhwa Jung, Richard D. Piner, Sung Jin An, Xuesong Li, Aruna Velamakanni, Rodney S. Ruoff, (2009) Colloidal Suspensions of Highly Reduced Graphene Oxide in a Wide Variety of Organic Solvents *Nano Lett.*, *9* (4) 1593–1597.

[90] Chun Kiang Chua, Martin Pumera, (2014), Chemical reduction of graphene oxide: a synthetic chemistry viewpoint *Chem. Soc. Rev.*, *43* 291.

[91] I. Moon, J. Lee, R. Ruoff, H. Lee, (2010). *Nat. Commun.*, *1*.

[92] Hannes C. Schniepp, Je-Luen Li, Michael J. McAllister, Hiroaki Sai, Margarita Herrera-Alonso, Douglas H. Adamson, Robert K. Prud'homme, Roberto Car, Dudley A. Saville, and Ilhan A. Aksay (2006) Functionalized Single Graphene Sheets Derived from Splitting Graphite Oxide *J. Phys. Chem. B,*, *110* (17) 8535–8539.

[93] Wu T, Liu S, Li H, Wang L, Sun X J (2011) Production of reduced graphene oxide by UV irradiation. *Nanosci Nanotechnol*, *11* (11) 10078–81.

[94] Yong Zhou , Qiaoliang Bao , Lena Ai Ling Tang ,Yulin Zhong and Kian Ping Loh, (2009) Hydrothermal Dehydration for the Green Reduction of Exfoliated Graphene Oxide to Graphene and Demonstration of Tunable Optical Limiting Properties. *Chem. Mater.*, *21* (13) 2950–2956.

[95] Xiaosi Zhou, Li-Jun Wan andYu-Guo Guo (2013) Binding SnO2 Nanocrystals in Nitrogen-Doped Graphene Sheets as Anode Materials for Lithium-Ion Batteries *Adv. Mater.*, *25* (15) 2152–2157.

[96] H. Shin, K. Kim, A. Benayad, S. Yoon, H. Park, I. Jung, M. Jin, H. Jeong, J. Kim, J. Choi, Y. Lee, (2009) 1987e1992. *Adv. Funct. Mater.*, *19* 1987–1992.

[97] C.-Y. Su, Y. Xu, W. Zhang, J. Zhao, A. Liu, X. Tang, C.-H. Tsai, Y. Huang, L.-J. Li, (2010). *ACS Nano.*, *4* 5285–5292.

[98] X. Fan, W. Peng, Y. Li, X. Li, S. Wang, G. Zhang, F. Zhang, (2008) Deoxygenation of Exfoliated Graphite Oxide under Alkaline Conditions: A Green Route to Graphene Preparation. *Adv. Mater.*, *20* 4490–4493.

[99] J. Rourke, P. Pandey, J. Moore, M. Bates, I. Kinloch, R. Young, R.N. Wilson, (2011). *Angew. Chem. Int. Ed.*, *50* 3173–3177.

[100] Wang H. (2011) Electrical conductivity of Alkaline-reduced Graphene oxide. *Chem. Res. Chinese universities*, *27* (5) 857-861.

[101] Sanjaya D. Perera, (2012) Alkaline deoxygenated graphene oxide for supercapacitor applications: An effective green alternative for chemically reduced graphene. *Journal of Power Sources*, *215* 1–10.

[102] Dan Li, Marc B. Mller, Scott Gilje, Richard B. Kaner, Gordon G. Wallace (2008) Processable aqueous dispersions of graphene nanosheets. *Nature Nanotechnology*, *3* 101–105.

[103] X. Dong, C.-Y. Su, W. Zhang, J. Zhao, Q. Ling, W. Huang, P. Chen, L.-J. Li, (2010) *Phys. Chem. Chem. Phys.*, *12* 2164–2169.

[104] He H, Klinowski J, Forster M, Lerf AA (1998). *Chem Phys Lett*, *287*, 53.

[105] Lerf A, He H, Forster M, Klinowski J (1998). *J Phys Chem B*, *102* 4477.

[106] Stankovich S (2006). *J Mater Chem*, *16*, 15.

[107] Zangmeister CD (2010). *Chem Mater*, *22* 5625.

[108] Tien HW, Huang YL, Yang SY, Wang JY, Ma CCM (2011). 49:1550 *Carbon*, *49* 1550.

[109] A, Jia Y, Wu Y, Nguyen ST, Ruoff RS (2007). *Carbon*, *45* 1558.

[110] Cote LJ, Cruz-Silva R, Huang J (2009). *JACS*, *131* 11027.

[111] R. Giardi, S. Porro, A. Chiolerio, E. Celasco, M. Sangermano, (2013). *J. Mater. Sci.*, *48* 1249.

[112] M. Sangermano, S. Marchi, L. Valentini, S. BittoloBon, P. Fabbri, (2011). *Macromol. Mater. Eng.*, *296* 401.

[113] Yang D, Velamakanni A, Bozoklu G, Park S, Stoller M, Piner RD, Stankovich S, Jung I, Field DA, Ventrice CA Jr, Ruoff RS (2009). *Carbon*, *47*, 145.

[114] Yuxi Xu, Kaixuan Sheng, Chun Li, and Gaoquan Shi (2010) Self-Assembled Graphene Hydrogel via a One-Step Hydrothermal Process. *ACS Nano*, *4* (7), 4324–4330.

[115] Sangeetha, N. M.; Maitra, U. (2005) Supramolecular Gels: Functions and Uses. *Chem. Soc. Rev.*, *34* 821–836.

[116] Banerjee, S.; Das, R. K.; Maitra, U. (2009) Supramolecular Gels In Action. *J. Mater. Chem.*, *19*, 66496687.

[117] Lorna, M. F. A.; Gibson, (1997) J. Cellular Solids: Structure and Properties. *Cambridge University Press*, 93–98.

[170] Li Zhang and Gaoquan Shi, (2011) Preparation of Highly Conductive Graphene Hydrogels for Fabricating Supercapacitors with High Rate Capability. *J. Phys. Chem. C*, *115*, 17206–17212.

[119] H. Klauk, (2007). *Nat. Mater.*, *6*, 397.

[120] M. Singh, H.M. Haverinen, P. Dhagat, E.G. Jabbour, (2010). *Adv. Mater.*, *22*, 673.

[121] B.J. De Gans, P.C. Duineveld, U.S. Schubert, (2004). *Adv. Mater.*, *16*, 203.

[122] Perelaer J, Smith PJ, Mager D, Soltman D, Volkman SK, Subramanian V, Korvinkdf JG, Schubert US (2010). *J Mater Chem*, *20* (39), 8446.

[123] Cho J, Shin K, Jang J (2010). *Thin Solid Films*, *518*, 5066.

[124] Park BK, Kim D, Jeong S, Moon J, Kim JS (2007). *Thin Solid Films*, *515*, 7708.

[125] Chiolerio A, Cotto M, Pandolfi P, Martino P, Camarchia V, Pirola M, Ghione G (2012). *Microelectron Eng*, *97*, 8.

[126] Chiolerio A, Maccioni G, Martino P, Cotto M, Pandolfi P, Rivolo P, Ferrero S, Scaltrito L (2011). *Microelectron Eng*, *88*, 2481

[127] Chiolerio A, Vescovo L, Sangermano M (2010). *Macromol Chem Phys*, *211*, 2008.

[128] Chiolerio A, Sangermano M (2012). *Mater Sci Eng B*, *177*, 373.

[129] Valeton JJP, Hermans K, Bastiaansen CWM, Broer DJ, Perelaer J, Schubert US, Crawforde GP, Smith PJ (2010). *J Mater Chem*, *20* (3), 543.

[130] Magdassi S, Grouchko M, Berezin O, Kamyshny A (2010). *ACS Nano*, *4* (4), 1943.

[131] Sangermano M, Chiolerio A, Martino P (2012) *Macromol Mater and Eng.*, doi:10.1002/mame.201200072.

[132] Ling QD, Liaw DJ, Zhu C, Chan DSH, Kang ET, Neoh KG (2008). *Prog Polym Sci*, *33*, 917.

[133] Sangermano M, Bongiovanni R, Malucelli G, Priola A (2006) In: Bregg RK (ed) Horizons in polymer research. *Nova Science Publisher Inc.*, New York, 61.

[134] Bunde A, Havlin S (1996). *Fractals and disordered systems, 2nd edn.*, Springer, Berlin.

[135] Yoshioka Y, Calvert PD, Jabbour GE (2005). *Macromol Rapid Commun*, *26*, 238.

[136] Meixner RM, Cibis D, Krueger K, Goebel H (2008). *Micro-Syst Technol*, *14* (8), 1137.

[137] Jang D, Kim D, Moon J (2009). *Langmuir*, *25* (5), 2629.

[138] Tsai MH, Hwang WS, Chou HH, Hsieh PH (2008) 19(33):1 *Nanotechnol*, *19* (33), 1.

[139] Desie G, Allaman S, Lievens O, Anthonissen K, Soucemarianadin A (2002) Influence of substrate properties in drop and demand printing. *International Conference on Digital Printing Technologies.* , *1*, 360.

[140] Denneulin A, Bras J, Carcone F, Neuman C, Blayo A (2011). *Carbon*, *49*, 2603.

[141] Luechinger NA, Athanassiou EK, Stark WJ (2008). *Nanotechnol*, *19*, 445201.

[142] Shin KY, Hong JY, Jang J (2011). *Adv Mater*, *23*, 2113.

[143] Novoselov KS, Geim AK, Morozov SV, Jiang D, Katsnelson MI, Grigorieva IV, Dubon SV, Firsov AA (2005). *Nature*, *438*, 197.

[144] Novoselov KS, Jiang Z, Zhang Y, Morozov SV, Stormer HL, Zeitler U, Mann JC, Boebinger GS, Kim P, Geim AK (2007). *Science*, *315*, 1379.

[145] Wilson NR, Pandey PA, Beanland R, Young RJ, Kinloch IA, Gong L, Liu Z, Suenaga K, Rourke JP, York SJ, Sloan J (2009). *ACS Nano*, *3* (9), 2547.

[146] Kim H, Abdala AA, Makosko CW (2010) Graphene/polymer nanocomposites. *Macromol*, *43*, 6515.

[147] L.T. Le, M.H. Ervin, H. Qiu, B.E. Fuchs, W.Y. Lee, (2011). *Electrochem. Commun.*, *13*, 355.

[148] H. He, J. Klinowski, M. Forster, A.A. Lerf, (1998). *Chem. Phys. Lett.*, *287*, 53.

[149] A. Lerf, H. He, M. Forster, J. Klinowski, (1998). *J. Phys. Chem. B*, 4477.

[150] D. Yang, A. Velamakanni, G. Bozoklu, S. Park, M. Stoller, R.D. Piner, S. Stankovich, I. Jung, D.A. Field, C.A. Ventrice Jr, R.S. Ruoff, (2009). *Carbon*, *47*, 145.

[151] M. Sangermano, S. Marchi, L. Valentini, S. BittoloBon, P. Fabbri, (2011). *Macromol. Mater. Eng.*, *296*, 401.

[152] S. Bocchini, A. Chiolerio, S. Porro, D. Accardo, N. Garino, K. Bejtka, D. Perrone, C.F. Pirri, (2013). *J. Mater. Chem.*, *1*, 5101.

[153] Chiolerio, A., Bocchini, S., Porro, S. (2014). *Adv. Funct. Mater.*, doi: 10.1002/adfm.201303371.

[154] BP Startistical Review of World Energy, June 2014, www.bp.com/statisticalreview.

[155] U.S. Energy Information Administration (EIA), International Energy Outlook 2013, www.eia.gov/forecasts/ieo/pdf/0484(2013).pdf

[156] A.K. Shukla, A. Banerjee, M.K. Ravikumar, A. Jalajakshi, (2012) Electrochemical capacitors: Technical challenges and prognosis for future Markets. *Electrochimica Acta*, *84*, 165–173.

[157] A.G Pandolfo, A.F. Hollenkamp (2006) Carbon properties and their role in supercapacitors. *Journal of Power Sources*, *157*, 11–27.

[158] G. G. Wallace, J. Chen, D. Li, S. E. Moulton and J. M. Razal, (2010) Nanostructured carbon electrodes. *J. Mater. Chem.*, *20*, 3553–3562.

[159] Patrice Simon, Yury Gogotsi, (2008) Materials for electrochemical capacitors. *Nature materials*, *7*.

[160] US Department of Energy. (2007) Basic Research Needs for Electrical Energy Storage, www.sc.doe.gov/bes/ reports/abstracts.htmlEES2007

[161] Katsuhiko Naoi, Patrice Simon, (2008) New Materials and New Configurations for Advanced Electrochemical Capacitors. *The Electrochemical Society Interface*, *1*, 5101.

[162] V. L. Chevrier and G. Ceder, (2011) Challenges for Na-ion Negative Electrodes. *Journal of The Electrochemical Society*, *158* (9), A1011–A1014.

[163] Brian L. Ellis, Linda F. Nazar, (2012) Sodium and sodium-ion energy storage batteries. *Current Opinion in Solid State and Materials Science*, *16*, 168177.

[164] Simon Engelke, (2013) Current and future sodium-ion battery research. *Storage4*, *1*, 1.

[165] Katsuhiko Naoi, Wako Naoi, Shintaro Aoyagi, Jun-ichi Miyamoto, and Takeo Kamino, (2013) New Generation Nanohybrid Supercapacitor. *Acc. Chem. Res.*, *46*(5), 10751083.

[166] Yulong Liu, Hong Zhang, Pan Ouyang, Zhicheng Li, (2013) One-pot hydrothermal synthesized MoO2 with high reversible capacity for anode application in lithium ion battery. *Electrochimica Acta*, *102*, 429–435.

[167] Kuok Hau Seng, Guo Dong Du, Li Li, Zhi Xin Chenb Hua Kun Liu and Zai Ping Guo, (2012) Facile synthesis of graphene-molybdenum dioxide and its lithium storage properties. *J. Mater. Chem.*, *22*, 16072.

[168] Yun Xu, Ran Yi, Bin Yuan, Xiaofei Wu, Marco Dunwell, Qianglu Lin, Ling Fei, Shuguang Deng, Paul Andersen, Donghai Wang, and Hongmei Luo (2012) High Capacity MoO2/Graphite Oxide Composite Anode for Lithium- Ion Batteries. *J. Phys. Chem.Lett.*, *3*, 309–314.

[169] Dale A.C. Brownson, Dimitrios K. Kampouris, Craig E. Banks, (2011) An overview of graphene in energy production and storage applications. *Journal of Power Sources*, *196*, 4873–4885.

[170] Li Li Zhang, Rui Zhou, X. S. Zhao, (2010) Graphene-based materials as supercapacitor electrodes. *J. Mater. Chem.*, *20*, 5983-5992.

[171] Li Zhang and Gaoquan Shi (2011) Preparation of Highly Conductive Graphene Hydrogels for Fabricating Supercapacitors with High Rate Capability. *J. Phys. Chem. C*, *115*, 17206–17212.

[172] Sheng Kai-xuan, Xu Yu-xi, Li Chun, Shi Gao-quan, (2011) High-performance self-assembled graphene hydrogels prepared by chemical reduction of graphene oxide. *New Carbon Materials*, *26*(1), 9–15.

[189] Yongming Sun, Xianluo Hu, Wei Luo, and Yunhui Huang, (2011) Self-Assembled Hierarchical MoO2/Graphene Nanoarchitectures and Their Application as a High-Performance Anode Material for Lithium-Ion Batteries. *ACS Nano*, *5*(9), 71007107.

[174] Srirama Hariharan, Kuppan Saravanan, Palani Balaya, (2013) -MoO3: A high performance anode material for sodium-ion batteries. *Electrochemistry Communications*, *31*, 5–9.

[175] Torsten Brezesinski, John Wang, Sarah H. Tolbert, Bruce Dunn, (2010 )Ordered mesoporous -MoO3 with iso-oriented nanocrystalline walls for thin-film pseudocapacitors. *nature materials*, *9*.

[176] Lukman Noerochima, Jia-Zhao Wanga, David Wexlerc, Zhong Chaoa, and Hua-Kun Liua, (2013) Rapid synthesis of free-standing MoO3/ Graphene films by the microwave hydrothermal methodas cathode for bendable lithium batteries. *Journal of Power Sources*, *228*, 198–205.

[177] J.F. Moulder, J. Chastain, R.C. King, (1995) Handbook of X-ray Photoelectron Spectroscopy: A Reference Book of Standard Spectra for Identification and Interpretation of XPS Data. *Physical Electronics*, Eden Prairie, MN.

[178] X.Y. Chen, Z.J. Zhang, X.X. Li, C.W. Shi, X.L. Li, (2006) Selective synthesis of metastable MoO2 nanocrystallites through a solution-phase approach. *Chemical Physics Letters*, *418*, 105.

[179] Kuok Hau Seng, Guo Dong Du, Li Li, Zhi Xin Chen, Hua Kun Liu and Zai Ping Guo (2012) Facile synthesis of graphenemolybdenum dioxide and its lithium storage properties. *J. Mater. Chem.*, *22*, 16072.

[180] Khorasani, M. M.; Norouzifar, M.; Shahrousvand, H. (2010) A New Reduction Route for the Synthesis of Nanoscale Metals and Metal Oxides with Ascorbic Acid at Low Temperature. *J. Iran. Chem. Soc.*, *7*, 113122.

[181] Wang, S. T.; An, C. H.; Zhang, Y. G.; Zhang, Z. D.; Qian, Y. T. (2006) Ethanothermal Reduction to MoO2 Microspheres via Modified Pechini Method. *J. Cryst. Growth*, *293*, 209–215.

[182] Chen, J. L.; Burger, C.; Krishnan, C. V.; Chu, B. (2005) Morphogenesis of Highly Ordered Mixed-Valent Mesoporous Molybdenum Oxides. *J. Am. Chem. Soc.*, *127*, 14140–14141.

[183] I. Roppolo, A. Chiappone, K. Bejtka, E. Celasco, A. Chiodoni, F. Giorgis, M. Sangermano, S. Porro, (2014). *Carbon*, *77*, 226–235.

[184] F. Xia, X.Hu, Y.Sun, W. Luo and Y.Huang, (2012). *Nanoscale*, *4*, 4707–4711.

[185] Perkin-Elmer (1979) Handbook of Photoelectron Spectroscopy. *Physical Electronics Division*, Eden Prairie, MN, 112–13.

[186] R. B. Quincy, M. Houalla, A. Proctor, D. M. Hercules, (1990). *J. Phys. Chem.*, *94*(4), 1520–26.

[187] Y. Liu, H. Zhang, P. Ouyang, Z. Li (2013) *Electrochimica Acta*, *102*, 429-35.

[188] B. C. Gates, H. knoezinger, F. C. Jentoft, (2009). *Academic Press*, *52*, 306.

[189] Y. Sun, X. Hu, W. Luo, Y. Huang, (2012). *J. Mater. Chem.*, *22*, 425-31.

[190] Porro S, Musso S, Giorcelli M, Tagliaferro A, Dalal SH, Teo KBK, Jefferson DA, Milne WI (2006) Study of CNTs and nanographite grown by thermal CVD using different precursors. *J. Non-Crystalline Solids*, *352*, 1310-3.

[191] Rajeswari J, Kishore PS, Viswanathan B, Varadarajan TK (2009) One-dimensional MoO2 nanorods for supercapacitor applications. *Electrochemistry Communications*, *11*, 572-57.

[192] Yi YX, Yuan B, Wu X, Dunwell M, Lin Q, Fei L, Deng S, Andersen P, Wang D, Luo H. (2012) High capacity MoO2/graphite oxide composite anode for Li-ion batteries. *J. Phys. Chem. Lett.*, *3*, 309-14.

[193] Meryl D. Stoller and Rodney S. Ruoff, (2010) Best practice methods for determining an electrode materials performance for ultracapacitors. *Energy Environ. Sci.*, *3*, 1294–1301.

[194] Supercapacitors material systems and applications, G.Q Max Lu, (2013) Material for sustainable energy and development. *Wiley-VCH*, Weinheim, Germany.

[195] Y. Xu, R. Yi, B. Yuan, X. Wu,. M. Dunwell,. Q. Lin,. L. Fei,. S. Deng, P. Andersen, D.Wang, H. Luo, (2012). *J. Chem. Lett.*, *3*, 309-14.

[196] I. A. Courtney, J. R. Dahn, (1997). *J. Electrochem. Soc.*, *144*, 2045–2052.

[197] M. D. Stoller, R. S. Ruoff (2010). *Energy and Environmental Science*, *3*, 1294–1301.

[198] Lu GQM, Beguin F, Frackowiak E. (2013) Supercapacitors: materials, systems and applications. *Wiley-VCH*, Weinheim Germany:

[199] Yu A, Chabot V, Zhang J. (2013) Electrochemical Supercapacitors for Energy Storage and Delivery: Fundamentals and Applications. *CRC Press*, Vancouver, Canada.

[200] Donghai Wang, Daiwon Choi, Juan Li, Zhenguo Yang, Zimin Nie, Rong Kou, Dehong Hu, Chongmin Wang, Laxmikant V. Saraf, Jiguang Zhang, Ilhan A. Aksay, and Jun Liu,(2009) Self-Assembled TiO2Graphene Hybrid Nanostructures for Enhanced Li-Ion Insertion. *ACS Nano*, *3* (4), 907–914.

[201] Zheye Zhang, Fei Xiao, Yunlong Guo, Shuai Wang, and Yunqi Liu (2013) One-Pot Self-Assembled Three-Dimensional TiO2Graphene Hydrogel with Improved Adsorption Capacities and Photocatalytic and Electrochemical Activities. *ACS Appl. Mater. Interfaces*, *5* 22272233.

[202] Hui Xiong, Michael D. Slater, Mahalingam Balasubramanian, Christopher S. Johnson, and Tijana Rajh,(2011) Amorphous TiO2 Nanotube Anode for Rechargeable Sodium Ion Batteries. *J. Phys. Chem. Lett.*, *2*, 2560–2565.

[203] Ki-Tae Kim, Ghulam Ali, Kyung Yoon Chung, Chong Seung Yoon, Hitoshi Yashiro Yang-Kook Sun, Jun Lu, Khalil Amine, and Seung-Taek Myung, (2014) Anatase Titania Nanorods as an Intercalation Anode Material for Rechargeable Sodium Batteries. *Nano Lett.*, *14* (2), 416–422.

[204] Xuesong Li et al., (2009) Large-Area Synthesis of High-Quality and Uniform Graphene Films on Copper Foils. *Science*, *324* (5932), 1312–1314 .

[205] Z. H. Ni, H. M. Wang, J. Kasim, H. M. Fan, T. Yu, Y. H. Wu, Y. P. Feng, and Z. X. Shen, (2007) Graphene Thickness Determination Using Reflection and Contrast Spectroscopy. *Nano Lett.*, *7* (9).

[206] S. Ummartyotin, J. Juntaro, C. Wu, M. Sain, and H. Manuspiya, (2011) Deposition of PEDOT: PSS Nanoparticles as a Conductive Microlayer Anode in OLEDs Device by Desktop Inkjet Printer. *Journal of Nanomaterials*, http://dx.doi.org/10.1155/2011/606714.

[207] Cappella, B; Dietler, G (1999), Force-distance curves by atomic force microscopy. *Surface Science Reports*, *34*, 1–104. doi:10.1016/S0167-5729(99)00003-5.

[208] Tung, V.C er al., (2009). *Nat. nanotechnology*, *4*, 25–29.

[209] Jannik C. Meyer, A. K. Geim, M. I. Katsnelson, K. S. Novoselov, T. J. Booth, S. Roth , (2007), The structure of suspended graphene sheets. *Nature*, *446*, 60–63.

[210] Andrea C. Ferrari, (2007) Raman spectroscopy of graphene and graphite: Disorder, electronphonon coupling, doping and nonadiabatic effects. *Solid State Communications*, *143*, 47–57.

[211] Chun Kiang Chua and Martin Pumera, (2014) Chemical reduction of graphene oxide: a synthetic chemistry viewpoint. *Chem. Soc. Rev.*, *43*, 291.

[212] Y. Ding, Y. Jiang, F. Xu, J. Yin, H. Rea, Q. Zhuo, Z. Long, P. Zhang, (2010) Preparation of nano-structured LiFePO4/graphene composites by co-precipitation method. *Electrochemistry Communications*, *12* (1), 10–13.

[213] Baojun Li, Huaqiang Cao, Jin Shao, Meizhen Qu and Jamie H. Warner, (2011) Superparamagnetic Fe3O4 nanocrystals graphene composites for energy storage devices. *J. Mater. Chem.*, *21*, 5069–5075 .

[214] Hidefumi Hiura, Hisao Miyazaki and Kazuhito Tsukagoshi, (2010) Determination of the Number of Graphene Layers: Discrete Distribution of the Secondary Electron Intensity Derived from Individual Graphene Layers. *Appl. Phys. Express*, *3* 095101.

[215] Joseph Goldstein (2003). Scanning Electron Microscopy and X-Ray Microanalysis. Springer. ISBN 978-0-306-47292-3.

[216] R. F. Egerton (1996), Electron Energy Loss Spectroscopy in the Electron Microscope. 2nd ed., Plenum, New York, ISBN 0-306-45223-5..

[217] Zhu, M. et al., (2007) *Carbon*, *45* 2229–2234.

[218] Kim, K. et al, (2011) *ACS Nano*, *5* 2142–2146.

[219] Riedl et al., (2010) *J. Phys. D: Appl. Phys.*, *43* 374009 doi:10.1088/0022-3727/43/37/374009.

[220] Murugan, A. V.; Muraliganth, T.; Manthiram, A., (2009) *Chem. Mater.*, *21* 5004–5006.